Electron momentum distribution of icosahedral $Cd_{84}Yb_{16}$ studied by Compton scattering

J. T. Okada,* Y. Watanabe, and S. Nanao
Institute of Industrial Science, University of Tokyo, 4-6-1 Komaba, Meguro, Tokyo 153-8505, Japan

R. Tamura and S. Takeuchi
Department of Materials Science and Technology, Tokyo University of Science, 2641 Yamazaki, Noda, Chiba 278-8510, Japan

Y. Yokoyama
Himeji Institute of Technology, 2167 Shosha, Himeji 671-2201, Japan

N. Hiraoka,† M. Itou, and Y. Sakurai
Japan Synchrotron Radiation Research Institute (JASRI), SPring-8, 1-1-1 Kouto, Hyogo 679-5198, Japan
(Received 16 May 2003; published 27 October 2003)

The electron momentum distribution in icosahedral $Cd_{84}Yb_{16}$ has been studied using the high-resolution Compton scattering technique with a momentum resolution of 0.16 a.u. The experimental valence-electron Compton profile is decomposed into two components: an inverted parabolalike one and a broad Gaussian-like one. We have found that the Fermi sphere, deduced from the number of electrons under the inverted parabolalike component, just coincides with the quasi-Brillouin zones constructed from the intense (211111) and (221001) reciprocal points. The Gaussian-like part is attributed to the electron occupation of the Yb $5d$ states. These facts are taken as signature that both the Hume-Rothery mechanism and the sp-d hybridization mechanism contribute to the formation of the pseudogap, stabilizing the icosahedral phase of $Cd_{84}Yb_{16}$.

DOI: 10.1103/PhysRevB.68.132204 PACS number(s): 71.23.Ft, 78.70.Ck, 71.15.Ap

The existence of a pseudogap is one of the characteristic features in quasicrystals (QCs) and is believed to be of great importance in view of the cohesion mechanism of the unconventional materials.[1] The pseudogap forms in the density of states across the Fermi level E_F in two possible ways; one is the quasi-Brillouin zone (q-BZ)–Fermi sphere (FS) interaction, i.e., the Hume-Rothery mechanism, and the other is the sp-d hybridization. In the Hume-Rothery mechanism, strong Bragg reflection of electron wave functions causes a gap at E_F in the reciprocal space when the Fermi sphere touches the q-BZ. This mechanism works most effectively in icosahedral (i-) QCs since the q-BZs possess icosahedral symmetry, which is nearly spherical. Extensive investigations have revealed that QCs are stabilized at a fixed value of valence electrons-per-atom e/a. The diameter of the Fermi sphere, $2k_F$, is often estimated from the value of e/a based on a free-electron gas model using the Raynor's valency.[2] It is currently understood that, in some QCs, $2k_F$ is about the magnitudes of the reciprocal vectors giving intense Bragg reflections. In the hybridization mechanism for Al-transition metal (TM) QCs, the d states of a TM element are strongly hybridized with the s,p states from Al. The role of the sp-d hybridization in Al-TM Hume-Rothery alloys has been investigated by theoretical calculations[3–5]. These computations predict that the sp-d hybridization further enhances the depth and width of the pseudogap formed by the q-BZ–FS interaction. Experimentally, photoemission spectroscopy and soft-x-ray emission and absorption spectroscopy have confirmed that the sp-d hybridization plays a role in forming the pseudogap at E_F.[6,7]

Recently, new stable i-QCs have been found in binary Cd-Yb and Cd-Ca systems.[8,9] The QC phases were originally identified as unknown phases in the phase diagrams existing in the vicinity of the cubic crystalline phases, Cd_6M (M = Yb, Ca). Unlike the ternary QCs, the entropy term due to chemical disorder is of far less importance for the stability of the binary QCs, which makes the interpretation of the cohesion mechanism simpler in these QCs. The pseudogap features have been observed in the ultra-high-resolution photoemission spectra of i-$Cd_{5.7}Yb$ and cubic Cd_6Yb.[10] Until now, the stable i-QCs have been considered as Hume-Rothery electron compounds, since all the stable i-QCs form at fixed values of e/a. The value of e/a is 1.75 for Al-TM group and 2.1 for the Al-Zn-Mg group. Assuming that the valence values for Cd, Yb, and Ca are 2 [i.e., $(5s)^2$ for Cd, $(6s)^2$ for Yb, and $(4s)^2$ for Ca are treated as the valence electrons], the value of e/a for the QCs amounts to 2. However, the value of $2k_F$, estimated from the value of e/a, is larger than the size of the q-BZs constructed from the dominant (211111) and (221001) reflections. This implies that the Hume-Rothery mechanism does not work efficiently in the Cd-based QCs. Theoretically, Ishii and Fujiwara have investigated the cohesion mechanism of the 1/1 cubic approximants, Cd_6Yb and Cd_6Ca, using the tight-binding linear muffin-tin orbitals (TB-LMTO) method in the atomic-sphere approximation.[11] They have concluded that the hybridization of the Yb $5d$ states with the Cd $5p$ states plays a principal role in the formation of the pseudogap, while the Hume-Rothery mechanism has a minor one.

In this work we have studied the electron momentum distribution (Compton profile) of i-$Cd_{84}Yb_{16}$ obtained by the high-resolution Compton scattering technique. By analyzing the valence-electron part of the Compton profile, we show the possibility that both the predicted sp-d hybridization and the Hume-Rothery mechanism contribute to the formation of the pseudogap in the Cd-based QC.

In a Compton scattering experiment one obtains the so-called Compton profile,[12–14]

$$J(p_z) = \int \int n(\mathbf{p}) \mathrm{d}p_x \mathrm{d}p_y , \tag{1}$$

where $n(\mathbf{p})$ is the ground-state electron momentum density. In an independent-particle model, the momentum density is given by

$$n(\mathbf{p}) = \sum_i |\psi_i(\mathbf{r}) \exp(i\mathbf{p}\cdot\mathbf{r}) \mathrm{d}r|^2, \tag{2}$$

where $\psi_i(\mathbf{r})$ is an electron wave function. The summation in Eq. (2) extends over all the occupied states. The area under the Compton profile gives the total number of electrons N,

$$\int_{-\infty}^{\infty} J(p_z) \mathrm{d}p_z = N. \tag{3}$$

When the profile is decomposed into two or more components reflecting different electronic states, the area under each component gives the number of electrons occupying that state.

Until now, the Compton scattering technique has been applied to i-Al_6Li_3Cu (Ref. 16) and decagonal (d-) $Al_{72}Ni_{12}Co_{16}$.[17] In both cases, a partial profile with a parabolalike shape has been observed in the valence-electron Compton profiles.[18] The partial profiles are isotropic and thus are well accounted for by the free-electron-like sp bands.[19] The diameter of the Fermi sphere has been estimated from the number of electrons under the parabolalike profile. Comparing the sizes between the Fermi sphere and the q-BZs, it has been concluded that the Hume-Rothery mechanism plays an important role in i-Al_6Li_3Cu but not in d-$Al_{72}Ni_{12}Co_{16}$.

Pure elements of Cd (99.9999%) and Yb (99.9%) with nominal composition $Cd_{5.7}Yb$ were melted in a molybdenum foil sealed in a quartz tube under argon atmosphere. The ingot was subsequently annealed at 673 K for 24 h to obtain a homogeneous and equilibrium phase. The phase purity of i-QC was confirmed by x-ray diffraction. The Compton scattering experiment was carried out at BL08W, SPring-8.[20] The reader is referred to Hiraoka *et al.*[21] for the details of the spectrometer. The energy of the incident x rays was 116 keV and the scattering angle was 165°. The experimental momentum resolution was 0.16 a.u. The data processing to deduce the Compton profile from the raw energy spectrum consists of the following procedures: background subtraction; and energy-dependent corrections for the Compton scattering cross-section, the absorption of incident and scattered x rays in the sample, the efficiency of the analyzer and the detector, and the double scattering. A Compton profile of single-grain i-$Al_{56}Li_{33}Cu_{11}$ produced by Czochralsky method[22] was also measured for comparison. Figure 1 shows the measured total-electron Compton profile (open circles) of i-$Cd_{84}Yb_{16}$, together with the theoretical core-electron profile (solid line). Here, $(1s)^2$-$(3d)^8(4s)^2(4p)^6(4d)^{10}$ for Cd and $(2s)^2$-$(5p)^6(4f)^{14}$ for Yb are treated as the core electrons. The Yb 1s electrons are not included since they do not contribute to the Compton scattering events under the present

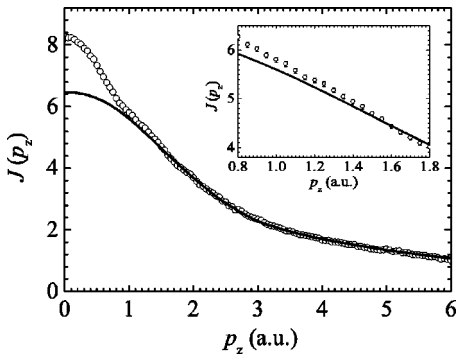

FIG. 1. Experimental Compton profile of total electrons (open circles) and theoretical core-electron Compton profile (solid line) in i-$Cd_{84}Yb_{16}$. The core-electron profile of each state is obtained from the data based on the free-atom Hartree-Fock calculations (Refs. 23) except for the Cd 4d state. The profile for Cd 4d electrons is calculated from the wave functions obtained by a FLAPW calculation on Cd metal. The experimental profile fits well into the core profile in the region of $|p_z| > 2.0$ a.u. In the region of 0.8 a.u.$< p_z <$1.6 a.u., there appears small difference between the two profiles as shown in the inset.

experimental conditions. The core-electron profile of each state is obtained from the theoretical data based on the free-atom Hartree-Fock calculations by Biggs *et al.*[23] except for the Cd $(4d)^{10}$ state. The profile of the $(4d)^{10}$ state was calculated from the 4d wave functions in Cd metal, since the 4d electrons in Cd_6Yb are considered to form a narrow band.[11] The 4d wave functions were computed using the full-potential linearized augmented plane-wave (FLAPW) method within the local-density approximation scheme.[24] As shown in Fig. 1, the experimental profile fits well into the theoretical core-electron profile in the region of $|p_z| > 2.0$ a.u. In the region of 0.8 a.u.$< |p_z| <$1.6 a.u., there appears small difference between the two profiles (see the inset of Fig. 1). In this connection, we made an extensive effort to analyze various corrections to the experimental data (i.e., multiple scattering, background subtraction, core-profile subtraction), but find our experimental results to be highly robust. Figure 2 presents the valence-electron Compton profile of i-$Cd_{84}Yb_{16}$, which is obtained by subtracting the theoretical core-electron profile from the experimental total-electron profile. The obtained valence-electron profile consists of two components: one is an inverted parabola in the region of $|p_z| < 0.9$ a.u. and the other is a broad Gaussian-like part extending to $|p_z| = 1.8$ a.u. This finding is different from that in i-$Al_{56}Li_{33}Cu_{11}$. The inset of Fig. 2 presents the experimental valence-electron Compton profile of i-$Al_{56}Li_{33}Cu_{11}$, where $(1s)^2$-$(2p)^6$ for Al, $(1s)^2$ for Li, and $(1s)^2$-$(3d)^{10}$ for Cu are treated as the core electrons. Although the remaining orbitals, which are treated as the valence electrons, are s, p states in the same way to i-$Cd_{84}Yb_{16}$, the profile of i-$Al_{56}Li_{33}Cu_{11}$ has a single parabolalike component. Theoretically, it has been reported that the pseudogap opening of 1/1-$Al_{52.5}Li_{32.5}Cu_{15}$ approximant is not due to the sp-d hybridization, but the interatomic hybridization between Al 3p states.[15] Experimentally, it has been shown that the Fermi sphere in i-Al_6Li_3Cu just touches the q-BZs formed by

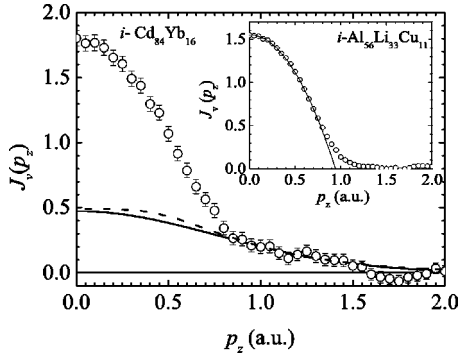

FIG. 2. Experimental valence-electron Compton profile (open circles) of i-$Cd_{84}Yb_{16}$. The experimental profile consists of two partial profiles: an inverted parabolalike profile and a broad Gaussian-like one. The dashed line shows the Lu $5d$ Compton profile computed from the data based on the free-atom Hartree-Fock calculations (Ref. 23). The solid line shows a Gaussian fitted to the experimental data in the range between 1.0 a.u. and 1.8 a.u. The inset shows the experimental valence-electron Compton profile of i-$Al_{56}Li_{33}Cu_{11}$, together with the fitted parabola (solid line). The Al-Li-Cu QC has only a single parabolalike profile in the valence-electron Compton profile.

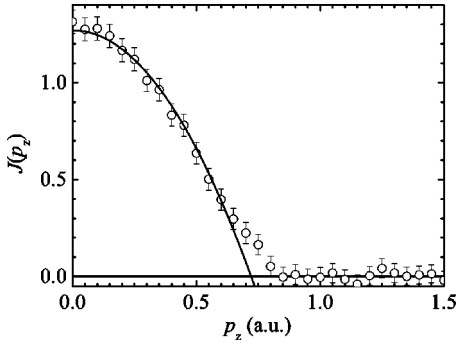

FIG. 3. Parabola-like part of the experimental valence-electron Compton profile (open circles) of i-$Cd_{84}Yb_{16}$, together with the fitted parabola (solid line).

dominant reflections.[16,25] Therefore, the existence of two components in i-$Cd_{84}Yb_{16}$ suggests that a mechanism other than the Hume-Rothery scenario also works for the pseudogap formation.

As shown in Fig. 2, the Gaussian-like part is well reproduced by the Compton profile of the atomic Lu $5d$ state (dashed line).[23] This fact implies that some of valence-electrons occupy the Yb $5d$ states in i-$Cd_{84}Yb_{16}$, since the shape of the Yb $5d$ profile is almost similar to that of the Lu $5d$ one. According to the TB-LMTO computations on cubic Cd_6M (M=Yb, Ca, Sr, Mg), the structural stabilization is obtained if M has a low-lying unoccupied d state.[11] The computations predict that the Yb $5d$ states are lowered below E_F by strong hybridization with the Cd $5p$ states.

Other possible causes of the Gaussian-like part are strong electron-electron and electron-lattice interactions. In an electron-gas model, the former produces a tail beyond the Fermi momentum in a Compton profile and the latter makes an addition to the tail with high-momentum components centered at reciprocal points due to the Umklapp processes.[19] A small tail is observed in the profile of i-$Al_{56}Li_{33}Cu_{11}$ (see the inset of Fig. 2) and in those of the previous experiments.[16,17] However, the Gaussian-like part in i-$Cd_{84}Yb_{16}$ is too large to be ascribed to the high-momentum tail due to the electron-electron and electron-lattice interactions.

Figure 3 shows the inverted parabolalike part of i-$Cd_{84}Yb_{16}$ (open circles), which is obtained by subtracting the Gaussian-like part from the valence-electron profile. Here, a Gaussian was fitted to the valence-electron profile in the range between $p_z=0.8$ a.u. and $p_z=1.6$ a.u. The fitted Gaussian (see the solid line in Fig. 2) was employed as the profile of the Gaussian-like part. In Fig. 3, the inverted parabolalike part is well reproduced by an inverted parabola (solid line) in the range from $p_z=0$ a.u. to $p_z=0.7$ a.u. This justifies the application of the electron-gas model for further discussion. The area under the inverted parabolalike part between $p_z=-1.0$ a.u. and $p_z=+1.0$ a.u. gives $e/a=1.26\pm0.14$ electrons. This value indicates that 0.74 electrons are transferred from the free-electron-like s, p bands into the Cd $5d$ states. From the value of e/a, the radius of the Fermi sphere, p_F, is calculated to be 0.63 ± 0.02 a.u. using the relation between p_F and the number of electrons n: $p_F=(3\pi^2 n)^{1/3}$. The result shows that the Fermi sphere just coincides with the q-BZs formed by the (211111) and (221001) reciprocal points (see Table I). Until now, it has been inferred that the radius of the Fermi sphere is 0.728 a.u. from $e/a=2$ and thus close to the sizes of the q-BZs constructed from the (222100) and (311111) reciprocal points. The present result shows that the Hume-Rothery mechanism should work more effectively than expected since the (211111) and (221001) Bragg diffraction are stronger than the (222100) and (311111) one.

As mentioned earlier, the entropy term due to chemical disorder is not effective for the stabilization of the binary i-Cd-Yb alloys. This means that a considerable energy gain associated with a deep pseudogap is essential to the stabilization. Therefore, the present experimental results imply that both the sp-d hybridization mechanism and the Hume-Rothery mechanism contribute simultaneously to the stability of i-$Cd_{84}Yb_{16}$ by forming the deep pseudogap.

In summary, the Compton profile of i-$Cd_{84}Yb_{16}$ has been measured using the high-resolution Compton scattering spectrometer at BL08W, SPring-8. The experimental valence-electron Compton profile is decomposed into two components: an inverted parabolalike one and a broad Gaussian-like one. The radius of the Fermi sphere is found to be 0.63 a.u., which is estimated from the number of electrons under

TABLE I. The multiplicity and intensity of the dominant Bragg diffraction planes, and the radius (q) of the inscribed sphere of the q-BZs corresponding to the Bragg diffraction planes (Ref. 9).

Index	Multiplicity	Intensity	q (a.u.)
211111	12	57	0.614
221001	30	100	0.646
222100	60	19	0.732
311111	12	15	0.760

the inverted parabolalike component. The Fermi sphere just coincides with the q-BZs constructed from the most intense (211111) and (221001) reciprocal points, giving rise to a strong Hume-Rothery stabilization. On the other hand, the broad Gaussian-like component is ascribed to the presence of the Yb $5d$ states below E_F, which appears to be a consequence of theoretically predicted bonding states due to hybridization between the Yb $5d$ and Cd $5p$ states. Finally, it is inferred that both the Hume-Rothery mechanism and the sp-d hybridization mechanism play important roles in forming a deep pseudogap, stabilizing the icosahedral phase in the Cd-Yb binary alloys.

We are grateful to Y. Ishii for illuminating discussions. The Compton profile measurements were performed with the approval of JASRI (Proposal No. 2001B0320-ND-np). This work was supported in part by a Grant-in-Aid from the Ministry of Education, Culture, Sports, Science and Technology of Japan, Iketani Science and Technology Foundation, and the Light Metal Educational Foundation, Inc.

*Present address: RIKEN Harima Institute, Institute of Physical and Chemical Research (RIKEN), 1-1-1 Kouto, Hyogo 679-5148, Japan.

†Present address: ESRF, BP 220, F-38043 Grenoble Cedex, France.

[1] *Physical Properties of Quasicrystals*, edited by Z. M. Stadnik (Springer-Verlag, Berlin, 1999).

[2] G. V. Raynor, in *Progress in Metal Physics*, edited by B. Chalmers (Butterworths Scientific Publications, London, 1949), p. 1.

[3] J. Friedel, Helv. Phys. Acta **61**, 538 (1988).

[4] T. Fujiwara and T. Yokokawa, Phys. Rev. Lett. **66**, 333 (1991).

[5] G. Trambly de Laissardière, D.N. Manh, L. Magaud, J.P. Julien, F. Cyrot-Lackmann, and D. Mayou, Phys. Rev. B **52**, 7920 (1995).

[6] Z.M. Stadnik, D. Purdie, M. Garnier, Y. Baer, A.P. Tsai, A. Inoue, K. Edagawa, S. Takeuchi, and K.H.J. Buschow, Phys. Rev. B **55**, 10 938 (1998).

[7] V. Fournée, E. Belin-Ferré, and J.M. Dubois, J. Phys.: Condens. Matter **10**, 4231 (1998).

[8] A.P. Tsai, J.Q. Guo, E. Abe, H. Takakura, and T.J. Sato, Nature (London) **408**, 537 (2000).

[9] J.Q. Guo, E. Abe, and A.P. Tsai, Phys. Rev. B **62**, R14 605 (2000).

[10] R. Tamura, Y. Murao, S. Takeuchi, T. Kiss, T. Yokoya, and S. Shin, Phys. Rev. B **65**, 224207 (2002).

[11] Y. Ishii and T. Fujiwara, Phys. Rev. Lett. **87**, 206408 (2001).

[12] See, e.g., *Compton Scattering*, edited by B. Williams (McGraw-Hill, London, 1977).

[13] M.J. Cooper, Rep. Prog. Phys. **48**, 415 (1985).

[14] N. Shiotani, Jpn. J. Appl. Phys., Part 1 **38**, 18 (1999).

[15] U. Mizutani, T. Takeuchi, and H. Sato, J. Non-Cryst. Solids (to be published).

[16] Y. Tanaka, Y. Sakurai, S. Nanao, N. Shiotani, M. Ito, N. Sakai, H. Kawata, and T. Iwazumi, J. Phys. Soc. Jpn. **63**, 3349 (1994).

[17] J.T. Okada, Y. Watanabe, Y. Yokoyama, N. Hiraoka, M. Itou, Y. Sakurai, and S. Nanao, J. Phys.: Condens. Matter **14**, L43 (2002).

[18] Very recently, we have measured the Compton profiles of i-$Al_64Cu_23Fe_{13}$, i-$Al_64Cu_23Ru_{13}$, i-$Al_70Pd_20Mn_{10}$, and d-$Al_65Cu_15Co_{20}$, and found that there is a free-electron-like partial profile in the valence-electron Compton profiles of these QCs.

[19] P. Eisenberger, L. Lam, P.M. Platzman, and P. Schmidt, Phys. Rev. B **6**, 3671 (1972).

[20] Y. Sakurai, J. Synchrotron Radiat. **5**, 208 (1998).

[21] N. Hiraoka, M. Itou, T. Ohata, M. Mizumaki, Y. Sakurai, and N. Sakai, J. Synchrotron Radiat. **8**, 26 (2001).

[22] Y. Yokoyama, K. Fukaura, H. Sunada, R. Note, T. Sato, K. Hirga, A. Inoue and U. Mizutani, Mater. Trans., JIM **41**, 522 (2000).

[23] F. Biggs, L.B. Mendelsohn, and J.B. Mann, At. Data Nucl. Data Tables **16**, 201 (1975).

[24] Kodama, Hamada, and Yanase, Computer code BANDS01 (Fuji Research Institute Co., Ltd.).

[25] Y. Tanaka, S. Nanao, and S. Tanigawa, J. Phys.: Condens. Matter **9**, 11 247 (1997).